

$\Lambda(1405)$ observations in p+p and K^- -induced reactions

L. Fabbietti, K. Piscicchia, A. Scordo

Received: date / Accepted: date

Abstract The $\Lambda(1405)$ production in p+p collisions at 3.5 GeV and K^- -induced reactions is discussed. The shift of the measured spectral function of the $\Lambda(1405)$ in p+p reactions does not match either theoretical calculations for p+p reactions or experimental observation in previous K^- -induced reactions. New experiments with stopped and in-flight K^- are needed to study this initial state more in detail. The state of the art of the analysis is discussed.

1 Introduction

Lying slightly below the $\bar{K} - N$ threshold ($\approx 30 \text{ MeV}/c^2$), the broad $\Lambda(1405)$ resonance is considered to be linked to the antikaon-nucleon interaction. Hence the understanding of this resonance is mandatory to address the issue of the interaction. From a theoretical point of view the $\Lambda(1405)$ is treated within a coupled channel approach, based on chiral dynamics, in which the low-energy $\bar{K} - N$ interaction can be handled [1]. In this Ansatz the $\Lambda(1405)$ appears naturally as a dynamically generated resonance, resulting from the superposition of two components: a quasi-bound $\bar{K} - N$ state and a $\Sigma\pi$ resonance.

At present, the molecule-like character of the $\Lambda(1405)$ is commonly accepted.

L.Fabbietti

E12, Physik Department Technische Universitt Mnchen, Germany

Excellence Cluster "Origin and Structure of the Universe", Technische Universitt Mnchen, Garching, Germany

E-mail: laura.fabbietti@ph.tum.de

K. Piscicchia

INFN, Laboratori Nazionali di Frascati, Frascati (Rome), Italy

Centro Fermi - Museo Storico della Fisica e Centro Studi e Ricerche "Enrico Fermi", (Rome), Italy

E-mail: kristian.piscicchia@gmail.com

A. Scordo

INFN, Laboratori Nazionali di Frascati, Frascati (Roma), Italy

E-mail: alessandro.scordo@lnf.infn.it

However, the contribution of the $\Sigma\pi$ channel to the formation process is still discussed controversially.

In general, models can be constrained above the $\bar{K} - N$ threshold by K^-p scattering data and by the measurements of the $\bar{K}p$, $\bar{K}n$ scattering lengths extracted from kaonic atoms [2,3]. Below threshold, the only experimental observable related to the $\bar{K} - N$ interaction is the $\Lambda(1405)$ spectral shape extracted from the decays $\Lambda(1405) \rightarrow \approx 100\%(\pi\Sigma)^0$. In this work the measurements of the $\Lambda(1405)$ spectral function extracted from p+p collisions at 3.5 GeV measured by HADES at GSI and the ongoing analysis of the data collected with the KLOE apparatus at DAΦNE [4] for kaon-induced reactions are discussed. p+p collisions represent a rather complicated initial condition for the detailed calculation of the $\Lambda(1405)$ production and moreover the data published by the HADES collaboration [5,6,7] refer to the decays $\Lambda \rightarrow \Sigma^\pm$ where the contribution of the $\Sigma(1385)^0$ [8,9] can not be filtered out.

The $\Lambda(1405)$ production in $\bar{K}N$ reactions is of particular interest due to the prediction, in chiral unitary models [1], of two poles emerging in the scattering amplitude (with $S = -1$ and $I = 0$) in the region of the $\Lambda(1405)$ mass. One pole is located at higher energy with a narrow width, and is mainly coupled to the $\bar{K}N$ channel, while a second lower mass and broader pole is dominantly coupled to the $\Sigma\pi$ channel [10]. Both contribute to the final experimental invariant mass distribution [11,12]. Moreover, the $\Sigma^0\pi^0$ channel, which is free from the $I = 1$ contribution and from the isospin interference term, represents the golden decay channel for such state. One therefore expects two very different spectral function for the measured $\Lambda(1405)$ when employing proton or kaon beams. In this work we revise the results published by the HADES collaboration where the $\Lambda(1405)$ was measured in p+p collisions at 3.5 GeV and we discuss the yet unpublished data measured with KLOE and stopped/in-flight antikaons impinging on carbon and helium targets.

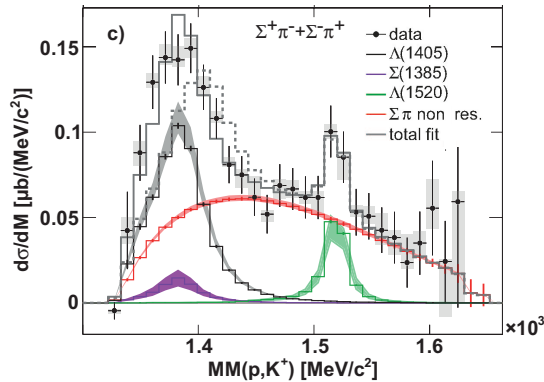


Fig. 1 (Color online) Missing mass $MM(p, K^+)$ distributions for events attributed to the $\Sigma^+\pi^-$ and $\Sigma^-\pi^+$ decay channels [5]. See text for details.

2 Results from p+p collisions

The HADES experiment at GSI is a multipurpose spectrometer with a large geometrical acceptance around mid-rapidity for nucleon-nucleon and nucleus-nucleus collisions in a fixed target configuration at intermediate energies ($E_{\text{KIN}} = 1 - 3.5$ GeV/nucleon). Figure 1 shows the missing mass $MM(p, K^+)$ distributions for events containing additionally a $\Sigma^+\pi^-$ or a $\Sigma^-\pi^+$ pair [5] extracted from p+p collisions at 3.5 GeV beam kinetic energy and measured with the HADES spectrometer. The intermediate Σ^+ and Σ^- hyperons have been reconstructed via the missing mass to the proton, the K^+ and either the π^- or the π^+ (see Fig. 4 in [13]). The details about the track reconstruction and particle identification are provided in [13, 5, 9]. The black symbols show the efficiency and acceptance corrected experimental data together with statistical and systematic errors (gray boxes), the black, violet and green continuous lines refer to the full scale simulation of the $\Lambda(1405)$, $\Sigma(1385)^0$ and $\Lambda(1520)$ production in the same final state, respectively. The $\Lambda(1405)$ has been simulated assuming a Breit-Wigner mass distribution peaked at 1385 MeV/ c^2 and with a width of 50 MeV/ c^2 , the nominal PDG mass values have been used for the $\Sigma(1385)^0$ and $\Lambda(1520)$. The red line shows the simulation of the non-resonant contribution of the same final state. The grey line represents the sum of these simulations and reproduces the experimental data very well. When simulating the $\Lambda(1405)$ with a Breit-Wigner distribution peaking at 1405 MeV/ c^2 and leaving all the other components unvaried, the resulting sum of the simulated channels is represented by the grey dashed line. One can see that this assumption is not compatible with the experimental data. The limited statistics of these data doesn't allow to distinguish between a Breit-Wigner and a Flatté distribution for the $\Lambda(1405)$, despite of the fact that the latter function is more suited for the description of a molecular state.

The differences expected in the spectral shapes of the $\Lambda(1405)$ reconstructed from the three decay channels $\Sigma^+\pi^-$, $\Sigma^-\pi^+$, $\Sigma^0\pi^0$ are not visible when comparing the two charged states measured by HADES (Fig. 1 in [5]). Also we know that the interference terms between the I=0 and I=1 states cancel out in the sum of the two charged amplitudes and that the remaining squared I=0 amplitude is dominant with respect to the squared I=1 amplitude. This way, the sum of the $\Sigma^+\pi^-$ and $\Sigma^-\pi^+$ distributions should be equivalent to the $\Sigma^0\pi^0$ distribution. For this reason the sum of the two efficiency corrected charged decays of the $\Lambda(1405)$ measured by HADES can be compared to the results published by the ANKE collaboration [14] and the corresponding theoretical prediction [15] where the neutral decay of the $\Lambda(1405)$ has been considered ($\Lambda(1405) \rightarrow \Sigma^0\pi^0$). The neutral decays offers the big advantage that it doesn't contain any contribution from the $\Sigma^0(1385)$ overlapping with the $\Lambda(1405)$ spectral shape, since the $\Sigma(1385)^0$ cannot decay into $\Sigma^0\pi^0$ pairs due to isospin conservation rules. Figure 2 shows the comparison of the HADES data with the ANKE measurement and a theoretical calculation. In order to compare the HADES data to the ANKE data and to the calculation by Geng and Oset the simulated curves corresponding to the sources other

than the $\Lambda(1405)$ have been subtracted from the experimental missing mass $MM(p, K^+)$ distribution shown in Fig.1. This way, the pure $\Lambda(1405)$ spectral shape can be compared, under the assumption that no interferences occur among the different intermediate states. The subtracted HADES spectrum is shown in Fig. 2 (full blue circles) together with the ANKE data (empty black circles) and the calculation (dashed green lines). Only statistical errors are displayed and the two dashed curves correspond to two different values of the total production cross-section for the $\Lambda(1405)$ in p+p collisions with a beam momentum of $3.65 \text{ GeV}/c$ ($E_{KIN} = 2.83 \text{ GeV}$) of 4 and $5.4 \mu\text{b}$ respectively. Indeed a total cross-section of $4.5 \mu\text{b}$ for the $\Lambda(1405)$ has been estimated from the ANKE analysis [14].

The ANKE data are not efficiency-corrected but they have been compared to absolutely normalised theoretical calculation in [15], where conclusions on the $\Lambda(1405)$ line shape have also been drawn. In Fig. 2 the ANKE data are scaled such that the integral of the $\Sigma\pi$ invariant mass spectrum between 1320 and $1440 \text{ MeV}/c^2$ is the same as the integral obtained for the HADES distribution. The theoretical calculations are also scaled by the same factor. The different binning of the HADES and ANKE histograms is accounted for in the errors shown for the HADES distribution. It is clear that here only a qualitative comparison of the two spectral shapes is possible, since the spectra published by ANKE are not corrected for efficiency and the beam energies for the two experiments differ. It has also to be pointed out that the ANKE spectrum does not show any sign of the expected $\Lambda(1520)$, while the cross-section extracted for this state from the HADES data is about half of the $\Lambda(1405)$ production cross section [5]. One can see that the two experimental distributions are in reasonable agreement even if this comparison is only qualitative. One can also see that the Geng-Oset calculations fail to reproduce the HADES data but also are compatible with the ANKE distributions only because of the large

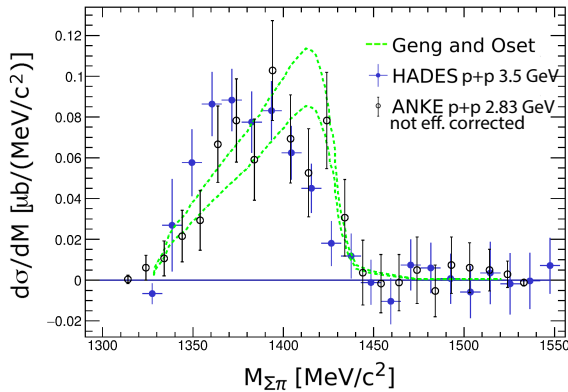


Fig. 2 (Color online) Missing mass $MM(p, K^+)$ distributions for events attributed to the HADES [5] and ANKE [14] data together with the $\Lambda(1405)$ spectral shape calculated in [15]. See text for details.

statistical error. A direct comparison would be only possible if a dedicated calculation for the charge decays of the $\Lambda(1405)$ produced in p+p collisions at 3.5 GeV kinetic energy would be available. Another crucial point is the presence of the non-resonant background, which is measured experimentally and might even interfere with the resonant contributions but is not considered yet in the calculation. Theoretical calculations as reported in [15] includes also the excitation of an intermediate $N^*(1710)$ but actually also other resonances could be excited and the non-resonant contribution should also be taken into account for the case of p+p collisions at 3.5 GeV. The comparison of the available data from p+p collisions suggest a shift of the $\Lambda(1405)$ pole mass towards lower value than the assumed nominal mass at 1405 MeV/c² but more detailed calculations should be carried out and compared to the data.

2.1 Kaon-induced reactions with AMADEUS

The AMADEUS experiment [16,17] has the aim to perform studies of the low energy hadronic interactions of negatively charged kaons with nucleons and nuclei, which are fundamental to solve longstanding open questions in the non-perturbative QCD strangeness sector. The experiment is located at the DAΦNE collider that provides a unique source of monochromatic low-momentum kaons stemming from the decay of the ϕ meson produced almost at rest within the $e^+ - e^-$ collider. The antikaons from the ϕ decay (BR \approx 50%) with a momentum of about 140 MeV/c can interact with the materials within the KLOE Drift Chamber (DC), that is used as an active target. This way, the DC provides an excellent acceptance and resolution data for K^- capture on H, ⁴He, ⁹Be and ¹²C, both at-rest and in-flight. The presence of a electromagnetic calorimeter surrounding the DC allows also for photon identification. Among the many physics topics that can be addressed within the AMADEUS program, the study of the $\Lambda(1405)$ spectral shape produced in in-flight and at-rest antikaon reactions on different target types is of crucial importance. In particular, the reconstruction of the decay $\Lambda(1405) \rightarrow \Sigma^0 \pi^0$ can be addressed thanks to the particle identification capability of KLOE. Data collected in 2005 have been analysed to study the spectral shape of the $\Lambda(1405)$ reconstructed in at-rest and in-flight reactions for K^- impinging on carbon, helium and hydrogen targets.

2.2 The $\Sigma^0 \pi^0$ identification

The selection of $\Sigma^0 \pi^0$ events proceeds, after the $\Lambda(1116)$ identification, with the search for three additional photon clusters in time coincidence with each other and stemming from the secondary decay vertex position reconstructed for the $\Lambda(1116)$ candidate (\mathbf{r}_Λ). To this end, a minimisation of the variable $\chi_t^2 = (t_i - t_j)^2 / \sigma_t^2$, where t_i represents the measured and corrected time of the i -th cluster, is performed to select three neutral clusters in the calorimeter

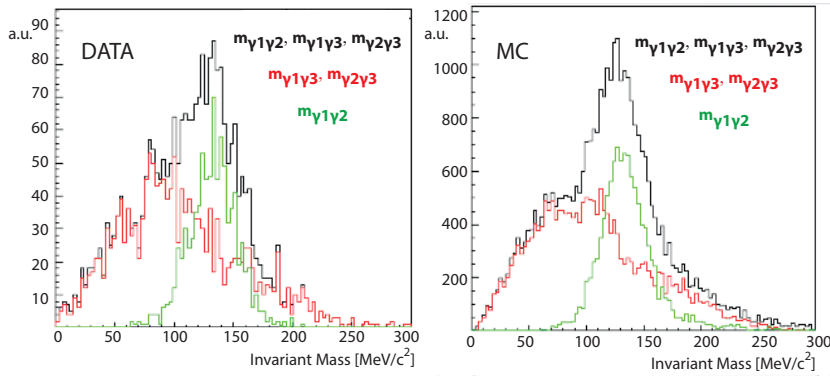


Fig. 3 (Color online) $m_{\gamma\gamma}$ invariant mass distribution from experimental and simulated data for events with a Σ^0 candidate. See text for details.

($E_{cl} > 20$ MeV). According to dedicated MC simulations a cut was optimised on this variable $\chi_t^2 \leq 20$.

Once the three photon cluster candidates are chosen, their assignment to the π^0 and Σ^0 decays is based on a second minimisation. Here, the variable $\chi_{\pi\Sigma}^2$ is used, that involves both the π^0 and Σ^0 masses. This variable is calculated for each possible combination and the minimising triplet is selected. This selection was optimised using MC simulations and the final selection corresponds to $\chi_{\pi\Sigma}^2 \leq 45$. According to true MC information the algorithm has an efficiency of $(98 \pm 1)\%$ in recognising photon clusters and an efficiency of $(78 \pm 1)\%$ in distinguishing the correct triplet. A check is performed on the clusters energy and distance to avoid the selection of split clusters (single clusters in the calorimeter erroneously recognised as two clusters) for π^0 s. Figure 3 shows the experimental and simulated invariant mass distribution for the photon pairs built from all the combination for the select minimising photon triplet. The green distributions in both panels show the invariant mass for the pair associated to the π^0 and the red curves correspond to the invariant mass of the other pairs. The black histogram represents the sum of all combinations within the minimising triplet. The γ_1 and γ_2 indexes indicate the two photons stemming from the π^0 decay, γ_3 refers to the photon associated to the Σ^0 decay. One can clearly see how the method allows for the reconstruction of the π^0 mass and also that the obtained experimental resolution is fairly well reproduced by the simulations. Figure 4 shows the invariant mass $m_{A\gamma_3}$ (for absorptions in the DC volume) together with a Gaussian fit that delivers a mean value and a width (σ) of 1193 and 15.65 MeV/ c^2 respectively. One of the major strengths of this analysis is the possibility of distinguish to a certain extend at-rest from in-flight reactions via the measurement of the momenta of the pion and Σ in the final state. The purity of this selection strongly depends on the reacting target, so that in some cases overlaps are presents and hence contemporary fits on different kinematic variables have to be employed. Figure 5 shows the pion versus Σ momentum distribution for the

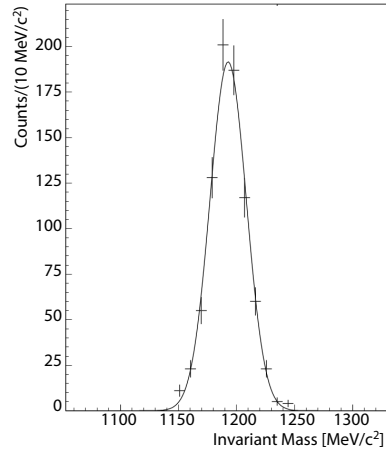


Fig. 4 (Color online) $m_{\Lambda\gamma 3}$ invariant mass distribution, together with a Gaussian fit.

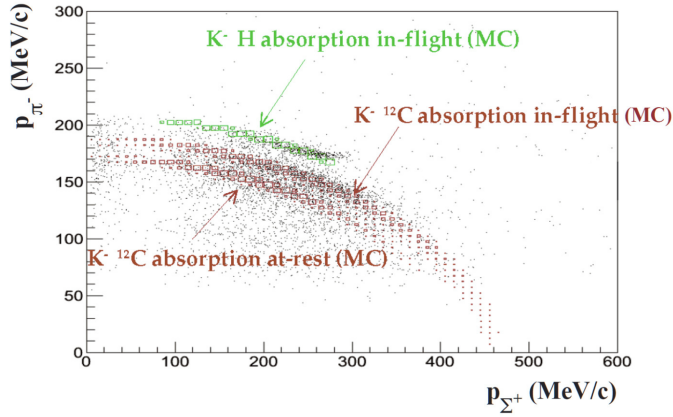


Fig. 5 (Color online) π^- momentum versus Σ^+ momentum. The black square represent the experimental distribution, the green symbol correspond to simulated $K^- + p$ at-rest reactions and the red symbols represent the simulated at-rest and in-flight reactions on carbon respectively.

selection of the two charged decay channels of the $\Lambda(1405)$. The experimental data are compared to full-scale simulation of at-rest and in-flight reaction on carbon (red symbols) and at-rest reactions on hydrogen (green symbols). One can see that the different bands obtained from the simulations are well distinguishable also in the experimental data. This example shows how the selection of the in-flight and at-rest reactions can be carried out. Preliminary results which are still under final evaluation show that the peculiarity of the in-flight reactions is that higher $\Lambda(1405)$ are accessible with respect to the at-rest reactions. Final results are to be expected soon. Since the measured $\Sigma^0\pi^0$ invariant mass distributions contain not only both the in-flight and at-

rest reactions leading to the $\Lambda(1405)$ formation on carbon and helium targets but also the non-resonant $\Sigma^0\pi^0$ production, a quantitative understanding of the underlying processes becomes mandatory. This requires appropriate calculations of antikaon reactions with carbon and helium nuclei including the correct treatment of spectator fragments and nucleons in order to describe the experimental momentum distribution correctly. This kind of calculation and comparison to the experimental data via full-scale simulations are currently ongoing.

3 Summary

We have discussed the $\Lambda(1405)$ results published by HADES comparing them directly to the ANKE measurement and the calculation by Geng and Oset, that are to this end the only available for the p+p initial conditions. The HADES data are rather compatible with the ANKE measurement, whereas a quantitative comparison is at this stage not possible since the ANKE data are not corrected for the geometrical acceptance and reconstruction efficiency. The presence of the non-resonant background in the experimental data calls for more extended calculation that could include all the contributing channels to the measured final states.

The feasibility of the measurement of the decay $\Lambda(1405) \rightarrow \Sigma^0\pi^0$ in reactions with monochromatic and low energy K^- beam on helium and carbon target has been shown. Together with the excellent particle identification the large acceptance of the KLOE spectrometer, employed in the phase 0 of the AMADEUS program, allows also to distinguish between in-flight and at-rest processes and to hence study the $\Lambda(1405)$ spectral shape in different kinematical conditions. A comparison of the obtained line shapes in the two reactions could help in better understanding the dynamic of the formation of the $\Lambda(1405)$ resonance.

References

1. N. Kaiser, P.B. Siegel, and W. Weise, Nucl. Phys. A594 (1995) 325; E. Oset and A. Ramos, Nucl. Phys. A635 (1998) 99; B. Borasoy, U.G. Meißner, and R. Nißler, Phys. Rev. C74 (2006) 055201; T. Hyodo and W. Weise, Phys. Rev. C77 (2008) 035204.
2. M. Bazzi et al. (SIDDHARTA Coll.), Phys. Lett. B704, 113 (2011).
3. Y. Ikeda, T. Hyodo, and W. Weise, Phys. Lett. B706, 63 (2011).
4. C. Curceanu et al., EPJ Web Conf. 66 (2014) 09004.
5. G. Agakishiev et al. (HADES coll.), Phys. Rev. C87 (2013) 025201.
6. J. Siebenson and L. Fabbietti, Phys. Rev. C88 (2013) 5, 055201.
7. G. Agakishiev et al. (HADES coll.), Nucl. Phys. A881 (2012) 178-186.
8. E. Epple and L. Fabbietti, Hyperfine Interact. 210 (2012) 45-51.
9. G. Agakishiev et al. (HADES coll.), Phys. Rev. C85 (2012) 0352013.
10. Y. Ikeda, T. Hyodo, W. Weise, Nucl. Phys. A881, (2012) 98.
11. J. A. Oller, U. G. Meissner, Phys. Lett. B500, (2001) 263.
12. J. C. Nacher, E. Oset, H. Toki, A. Ramos, Phys. Lett. B455 (1999) 55.
13. J. Siebenson et al. (HADES Coll.), AIP Conf. Proc. Vol. 1322, 389 (2010).
14. I. Zychor et al. (ANKE Coll.), Phys. Lett. B660, 167 (2008).
15. L. S. Geng and E. Oset, Eur. Phys. J. A34, 405 (2007).

-
16. AMADEUS Letter of Intent, http://www.lnf.infn.it/esperimenti/siddharta/LOI_AMDEUS_March2006.pdf
 17. The AMADEUS collaboration, LNF preprint, LNF/9607/24(IR) (2007)